



HAL
open science

AlGaN/GaN high electron mobility transistors on diamond substrate obtained through aluminum nitride bonding technology

Mahmoud Abou Daher, Marie Leseq, Pascal Tilmant, N. Defrance, Michel Rousseau, Yvon Cordier, Jean-Claude de Jaeger, Jean-Guy Tartarin

► To cite this version:

Mahmoud Abou Daher, Marie Leseq, Pascal Tilmant, N. Defrance, Michel Rousseau, et al.. Al-GaN/GaN high electron mobility transistors on diamond substrate obtained through aluminum nitride bonding technology. *Journal of Vacuum Science & Technology B, Nanotechnology and Microelectronics*, 2020, 38 (3), pp.033201. 10.1116/1.5143418 . hal-02929037

HAL Id: hal-02929037

<https://hal.science/hal-02929037>

Submitted on 11 Dec 2020

HAL is a multi-disciplinary open access archive for the deposit and dissemination of scientific research documents, whether they are published or not. The documents may come from teaching and research institutions in France or abroad, or from public or private research centers.

L'archive ouverte pluridisciplinaire **HAL**, est destinée au dépôt et à la diffusion de documents scientifiques de niveau recherche, publiés ou non, émanant des établissements d'enseignement et de recherche français ou étrangers, des laboratoires publics ou privés.

AlGaN/GaN HEMTs on Diamond Substrate obtained through Aluminum Nitride Bonding Technology

Running title: HEMT Transfer Technology

Running Authors: Abou Daher et al.

Mahmoud Abou Daher^{1, 3, a)}, Marie Lesecq¹, Pascal Tilmant¹, Nicolas Defrance¹, Michel Rousseau¹, Yvon Cordier², Jean Claude De Jaeger¹, Jean Guy Tartarin³

¹ Institut d'Electronique de Microélectronique et de Nanotechnologie (IEMN), UMR 8520, Université de Lille, Avenue Poincaré, BP60069, 59652 Villeneuve d'Ascq Cedex, France

² CRHEA-CNRS, Centre de Recherche sur l'Hétéro-Epitaxie et ses Applications, Rue Bernard Grégory, 06560 Valbonne, France

³ Laboratoire d'Analyse et d'Architecture des Systèmes (LAAS), 7 avenue du colonel Roche, 31031 Toulouse, France

a) Electronic mail: maboudah@laas.fr

The transfer technology is now becoming very attractive for new technologies such as flexible technology, but also for solid state technologies when the performances are limited by technological barriers that have to be overcome. In this last context, the transfer of High electron mobility transistors (HEMTs) on diamond substrate represents an opportunity to improve the thermal dissipation when the device operates at high radio frequency power levels. Up to now, the technological process for the transfer of these transistors was not detailed in the literature. In this letter, the first demonstration of AlGaN/GaN HEMTs on diamond substrate by transfer technology obtained through sputtered aluminum nitride (AlN) layers bonding at low temperature is reported. Devices are firstly fabricated on AlGaN/GaN epilayer grown on silicon (Si) substrate. Afterwards, AlGaN/GaN thin film with devices are released from the Si growth substrate and transferred at 160°C onto diamond substrate thanks to an AlN bonding layer. A full description of the transfer technology and all the technological limits and risks are presented. The transferred device

provides a maximum DC drain current density $I_{DS\ Max}$ of $690\text{ mA}\cdot\text{mm}^{-1}$ at $V_{GS} = 0\text{ V}$. Furthermore, a cutoff frequency f_T of 85 GHz and a maximum oscillation frequency f_{MAX} of 106 GHz are extracted from S-parameters measurement.

I. INTRODUCTION

Gallium Nitride (GaN) high electron mobility transistors are attractive devices for millimeter wave power applications. Most devices are fabricated by hetero-epitaxy either on Si substrate because of its low cost and large area availability, or on Silicon Carbide (SiC) substrate because of its good thermal properties and high resistivity. However, AlGaN/GaN HEMT growth on Si or SiC substrates require transition layers for lattice matching of the materials, that are responsible for many defects and that present a thermal barrier, thus limiting the thermal dissipation and the reliability¹⁻³ of the devices. To address the challenge regarding the heat dissipation enhancement, a possibility is to use a substitution substrate with high thermal conductivity such as diamond^{4,5}. Since the GaN layer direct growth on monocrystalline diamond substrate requires AlN nucleation layer⁶, efforts have focused on GaN HEMTs transferred onto synthetic diamond substrate. B. Lu and T. Palacios⁷ have demonstrated the transfer of AlGaN/GaN HEMTs from Si substrate to glass substrate using BenzoCycloButene (BCB) as adhesive layer. J-W. Chung et al. have demonstrated a transfer technique using Hydrogen-SilsesQuioxane (HSQ)⁸ as bonding layer. However, a high thermal annealing (400°C) is required to harden the HSQ layer, which can damage the devices. Furthermore, the BCB layer has a poor thermal conductivity (0.3 W/m. K), preventing the heat dissipation under power operation of HEMT. G. H. Jessen et al⁹ reported on AlGaN/GaN epilayer transferred onto a 25 μm -thick CVD diamond using atomic attachment. The epilayer transferred to CVD diamond

was then mounted to a Si wafer using a high temperature glass adhesive layer, in order to manufacture their devices. This last mount adds a thermal resistance between CVD Diamond and Si limiting the benefits of CVD diamond. P. Chao et al.¹⁰ have carried out the transfer from SiC substrate to polycrystalline diamond with a low thermal budget (< 150 ° C) through a thin Si-based adhesive layer, but the nature of the deposited layer for this transfer and the transfer technology itself was not detailed. T. Liu et al.¹¹ and Q. Wu et al.¹² have implemented other successful transfer methods from a monocrystalline SiC substrate to a polycrystalline diamond substrate, but without giving more details on the bonding layer, which represents the critical point for transfer technologies.

In this letter, a new technological transfer process based on the AlGaIn/GaN layer with devices released from Si growth substrate, and bonded at low temperature onto synthetic diamond substrate using sputtered AlN as adhesive layer is detailed. The technological limits and the risks of transfer technology are identified. Finally, the DC and RF electrical performances are presented for an AlGaIn/GaN HEMT with a gate length of 80 nm, transferred onto diamond substrate.

II. EXPERIMENTAL

In this section, the fabrication of HEMTs on Si substrate is firstly presented. Then, the transfer process overview depicted in figure 1 is detailed. AlN layer bonding technique with associated technological limits and risks are discussed.

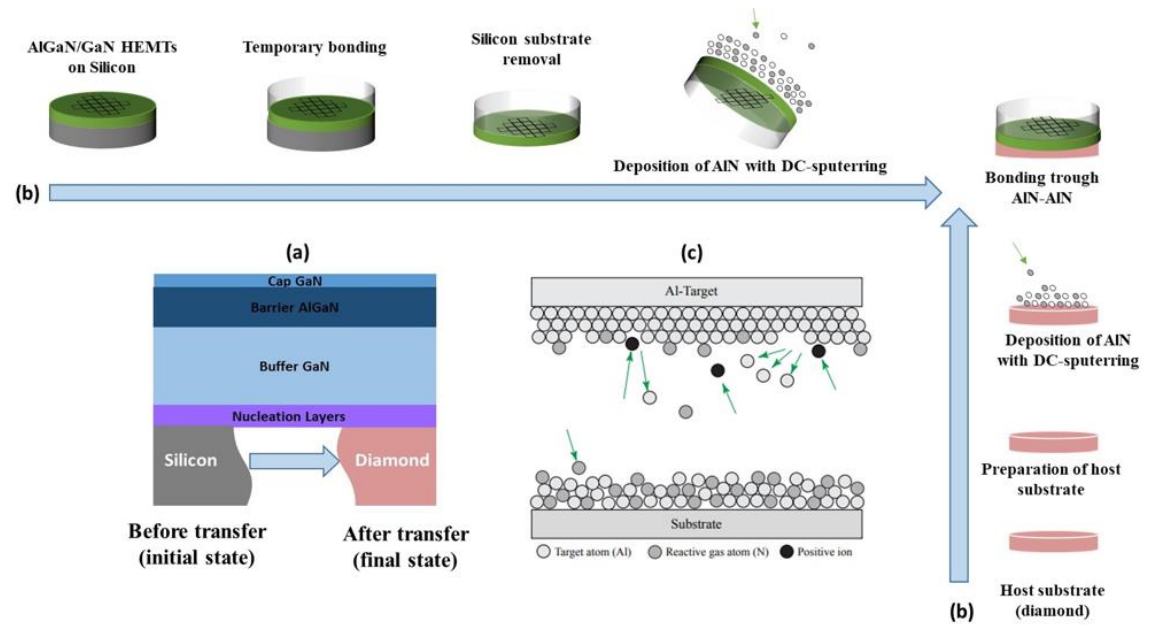


FIG. 1. (a) Structures before and after transfer, (b) Schematic overview of the method used in this work (c) Illustration of the reactive sputter process, where in this case the aluminum reacts with the nitrogen to form aluminum nitride bonding layer Reprinted with permission from F. Engelman, Doctoral dissertation of Philosophy in Solid State Electronics, Uppsala University, 23 (2002).

Copyright 2002 Uppsala University.

A. Device fabrication

Si is used as starting low cost substrate to grow the AlGa_N/Ga_N heterostructure. The MOCVD epitaxy consists of a 12.5 nm-thick AlGa_N barrier layer with an Al content of 26 %, a 2 nm AlN exclusion layer and a 1.6 μm Ga_N buffer grown on a stress mitigating stack on an AlN nucleation layer. The epilayer is protected by a 80 nm thick Si₃N₄ passivation layer deposited by Plasma Enhanced Chemical Vapor Deposition (PECVD). Transistors are processed with conventional and stable fabrication steps using e-beam lithography described elsewhere¹⁴. The fabrication starts with Ti/Al/Ni/Au (12/200/40/100 nm) ohmic contacts deposited by e-beam evaporation. This is followed by rapid thermal annealing (RTA) at 850 °C for 30 s. Devices are isolated by N⁺ ion multiple implantations.

The transistors feature a two-fingers configuration with several gate lengths ($L_g = 60$ nm; 70 nm and 80 nm), gate width ($W = 15$ μm ; 25 μm ; 35 μm ; 50 μm and 75 μm), and drain–source spacing ($L_{SD} = 1.5$ μm ; 2 μm and 2.5 μm). T-shape gates are patterned by electron-beam lithography process using optimized (PMMA/COPO/PMMA), tri-layer resist stack. The Schottky gate metal stack consists of evaporated Ni/Au (40/300 nm). This step is followed by an N_2O pretreatment for 2 min, and a passivation based on $\text{Si}_3\text{N}_4/\text{SiO}_2$ (50/100 nm) bilayer dielectric, performed by PECVD at 340 °C, leading to the mitigation of the surface states activity. Finally, the thick interconnection is processed by Ti/Au (100/400 nm) overlay metallization.

B. Transfer process overview description

Once HEMTs are fabricated on their growth Si substrate, the transfer process starts with the coating using a thick photoresist (AZ 4562) layer on the front side where transistors are processed before. This layer constitutes a protection for devices and is used as an adhesive layer to bond the front side of the devices onto a temporary glass carrier at 75°C for 1 hour. This glass wafer is especially dedicated for the use of lapping equipment and can be re-used several times to reduce the cost. Then, a step based on chemical mechanical lapping (CMP) is used to thin Si substrate down to 100 μm . The sample is then released from the glass substrate. Indeed, the glass substrate 1cm-thick and so not really convenient for the rest of the process. Thereby, the front side of the devices is bonded onto a sapphire substrate using a specific resist layer (AR-P 617-14) consistent with the following technological steps. The sapphire substrate is used as a temporary holder to etch the remaining 100 μm -thick Si layer using XeF_2 etching. This sapphire substrate can be

This is the author's peer reviewed, accepted manuscript. However, the online version of record will be different from this version once it has been copyedited and typeset.
PLEASE CITE THIS ARTICLE AS DOI: 10.1116/1.5143418

also re-used several times to limit the cost. A low etching rate ($4 \mu\text{m} \cdot \text{min}^{-1}$) is used to avoid the generation of cracks in the GaN layer due to stress evolution during the removal of the remaining different layers. The transparency of the GaN permits to see HEMTs via their back face as shown in Figure 2.



FIG. 2. Backside optical view (50 x) of HEMTs with low cracks in GaN layer after Si substrate removal.

The transfer process continues with the bonding step of backside devices onto diamond substrate, which has an area of 1 cm^2 . The choice of the adhesive layer is one of

the critical steps because its properties influence the performance of the components after transfer. For this purpose, AlN is chosen regarding its thermal conductivity (between 0.8 and 130 W/m. K for sputtered AlN layer depending on the film thickness, defect density and oxygen content ¹⁵⁻¹⁸). Furthermore, AlN layer permits to minimize the difference of the lattice parameter between the bonding layer and the nucleation layer. This AlN layer must also minimize the roughness of the diamond surface which is 50 nm, by filling the holes on the surface. These AlN layers are deposited by DC sputtering onto both parts to be assembled: diamond substrate from one side, and N-face GaN backside of the film with transistors on the other side. Various tests were performed to define the optimal deposition conditions to reduce and control the roughness and to achieve the best crystalline quality, by varying the temperature and the pressure deposition.

In agreement with the technological constraints (especially the presence of AR- P 617-14 resist layer as a bonding layer on top of the devices), the deposition temperature is set to 18 ° C under a pressure set at 4.7×10^{-3} mbar during 40 min. These conditions lead to an AlN layer thickness of 450nm (+/- 10 nm) at each side. Atomic Force Microscopy (AFM) measurement shows a roughness of 2.4 nm and 2.6 nm on the devices backside and on the diamond substrate respectively. These values are small enough to enable bonding. The bonding procedure consists in four steps described as follow:

A first annealing step for both films with transistors and diamond substrate is performed at 170 °C for 10 min under nitrogen flow in order to get rid of voids formation at the bonding interfaces.

Then, an Ar-based plasma activation is then performed on active film and diamond substrate to increase the hydrophilicity of the surfaces.

The active film and the diamond substrate are then rinsed with deionized water (DI H₂O), and dried under nitrogen flow.

Both surfaces of AlN are then put straightway in contact, making it possible to get an adherence between the active film of AlN layer on diamond substrate and AlN active layer on backside of our HEMTs by suction effect. AlN-AlN bonds are formed using a thermocompression bonding machine. A pressure of 650 mbar is applied on the stack of both parts and the ensemble is heated up to 160 °C for 3 h.

Finally, the front side resist layer is removed to release devices from the sapphire top substrate. Taking into account the modification of the resin properties following the different process steps, a specific solution based on a mix of N-Methyl-2-pyrrolidone, Dimethyl sulfoxide and Dichloromethane had to be used. Figure 3 shows a SEM image of a two-fingers configuration transistor transferred onto diamond substrate.

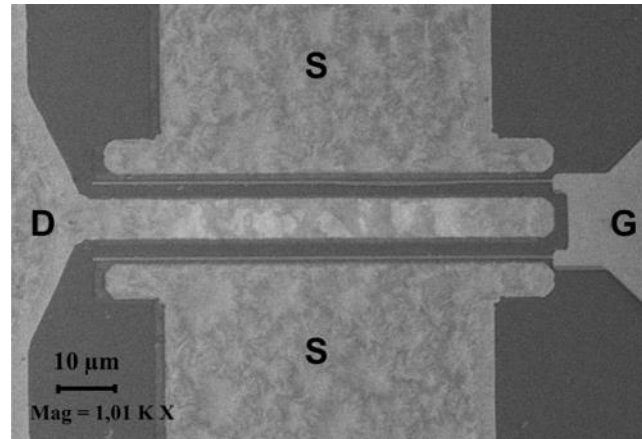


FIG. 3. SEM view of a $2 \times 75 \times 0.08 \mu\text{m}^2$ HEMT with a drain-source spacing $L_{SD} = 2.5 \mu\text{m}$ on diamond substrate after transfer process.

C. AlN Layer and bonding analysis

Figure 4 depicts the Scanning Electron Microscope (SEM) image of an AlN layer deposited by DC sputtering, revealing a columnar structure. The thickness of the AlN layer is measured to be 450 nm (± 10 nm). Energy-Dispersive X-ray Spectroscopy (EDS) analysis is performed on the AlN layer, revealing the presence of oxygen with a percentage of 11.6 %.

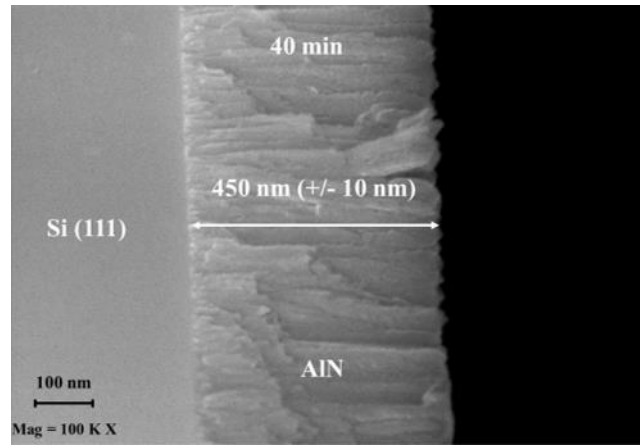


FIG. 4. SEM view of 450 nm (± 10 nm)-thick AlN layer deposited by DC-sputtering.

Figure 5(a) shows the Scanning Transmission Electronic Microscope (STEM) image of the bonding interface revealing the 100 nm-thick bonding ensemble. Figure 5(c) shows an Energy Dispersive Analysis (EDS) revealing an aluminum oxide interface layer with an atomic percentage of oxygen of 14 %. The correlation of the different colors (figure 5 b) permits to deduce an aluminum oxide layer represented by the yellow area. Based on EDS measurement and on the results published in ¹⁹, it can be deduced that the bonding interface is AlNO.

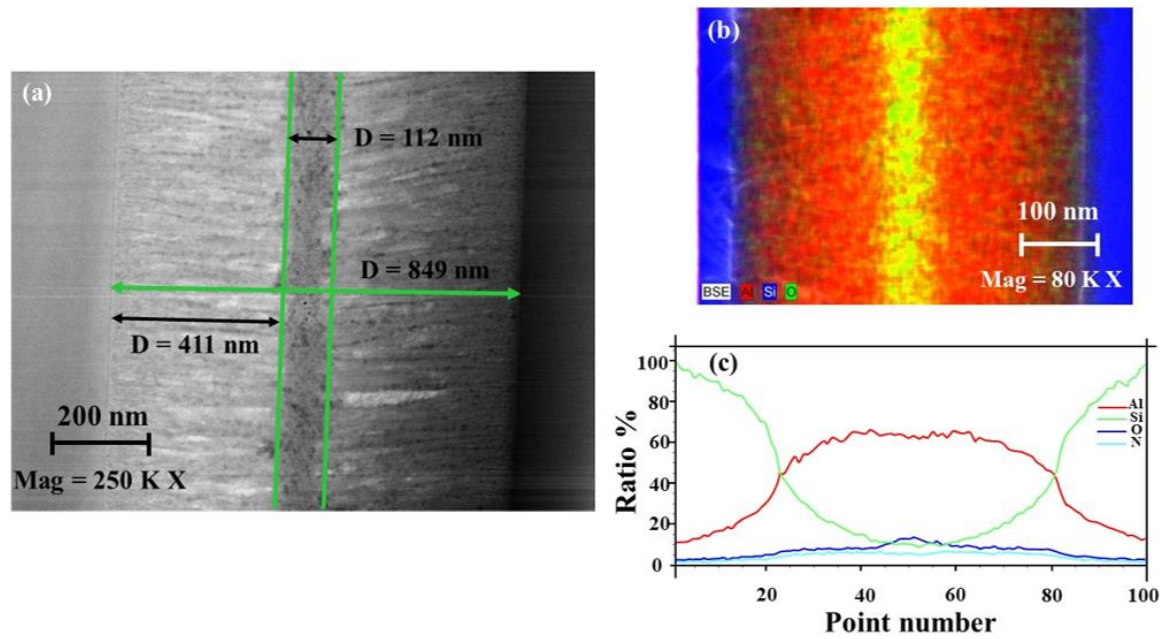


FIG. 5. STEM view of AlN-AlN interface (a), EDS image of interface (b), EDS analysis of interface (c).

D. Technological limits and risks

This original technological strategy has several limitations and risks that can be split into different types: Firstly, the transfer technology requires Si substrate etching, the selective etching of Si with the nitride materials like AlN, GaN, AlGa_{0.5}N can then relax the mechanical strains of our epitaxial layers. The stress relaxation effect in the AlGa_{0.5}N/GaN film has a significant limiting effect which can damage this film. Several Si etch tests have been done to control etching rate with XeF₂, which avoid the presence of cracks in GaN layer.

Secondly, the realization of the transfer requires the bonding of the components on an intermediate sapphire substrate through a resist layer. The choice of this resist layer must be compatible with the transfer procedure, especially the bonding temperature of AlN-AlN at 160°C and the XeF₂ etching. An optimization of the choice of the resist layer used was made in agreement with these limits. Several resist layers were tested in order to validate the transfer and lift-off of the components from intermediate substrate.

The third risk is the choice of AlN bonding layer between GaN and diamond was well detailed before. Several AlN deposit tests were made by varying the sputtering

temperature from 18 ° C to 150 ° C, in order to study the influence of this variation on crystalline quality and surface roughness. Morphological analysis by SEM, EDS and AFM were performed on these layers. The results showed that the crystalline quality did not vary much with this variation of sputtering temperature but the surface roughness of the AlN layers was degraded with the increase of sputtering temperature. Then, the deposition temperature was set at 18 ° C.

Furthermore, AlN layer is used to fill the holes present at the surface of the diamond substrate, as its surface roughness is around 50 nm. The critical thickness to validate this step with a minimum of surface roughness is evaluated around 400 nm, which explains our choice for the transfer validated by depositing 500 nm of AlN on diamond substrate.

In our process, up to now the nucleation layer of AlN that is between Si substrate and GaN buffer is kept. This layer limits the thermal dissipation towards the diamond substrate because of the dislocation and the thermal resistance of this layer.

In spite of all these limitations and risks that can damage the functionality of the HEMTs, the transfer of the transistors from Si to diamond substrate with this new detailed transfer technology was successful. New developments are however needed to push the concept further in terms of performances, and to validate the expected better reliability as a consequence of a better thermal management. In addition, to reach higher performance future studies will have to combine the improvement of heat dissipation and the improvement of crystal quality using conductive Si substrate for AlGaIn/GaN growth ²⁰. Since conductive silicon substrate will be removed for the transfer and so its electrical conductivity is no more a problem.

III. DC and RF characteristics

After the technological process of the HEMTs on Si substrate presented in part II. A, series of electrical DC characterization were performed. Then, after the first step of etching of Si substrate presented in part II. B, the same electrical measurements were performed. It was noticed that the electrical characteristics of the HEMTs before and after

back-thinning of the Si substrate down to $100\ \mu\text{m}$ are very similar but an improvement is observed after the HEMT transfer on the diamond substrate as it is described in the next section.

Figure 6 presents a comparison of the output I_{DS} (V_{DS}) characteristics of a HEMT featuring a two-fingers configuration with a gate length L_g of $80\ \text{nm}$ fabricated on Si substrate and the same HEMT transferred to diamond substrate. From these measurements, a maximum DC current density $I_{\text{DS Max}}$ of $690\ \text{mA}\cdot\text{mm}^{-1}$ is obtained at $V_{\text{GS}} = 0\text{V}$, associated with an ON-resistance of $2.1\ \Omega\cdot\text{mm}$ for HEMT on diamond substrate. The initial device on Si substrate featured a maximum DC current density $I_{\text{DS Max}}$ of $605\ \text{mA}\cdot\text{mm}^{-1}$ obtained at $V_{\text{GS}} = 0\text{V}$, associated with an ON-resistance of $2.5\ \Omega\cdot\text{mm}$. We notice a slight improvement of the maximum DC current density (+14%) and on the ON-resistance (-16%) after the transfer on diamond substrate, and the threshold voltage decreased from $V_{\text{th}} = -2\ \text{V}$ to $V_{\text{th}} = -3\ \text{V}$.

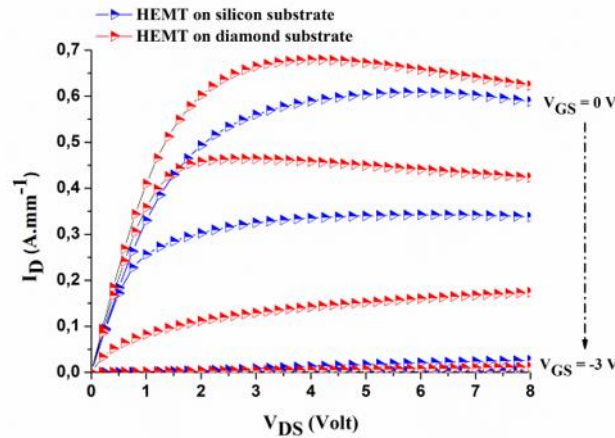


FIG. 6. I_{DS} (V_{DS}) DC output characteristics for a $2 \times 75 \times 0.08\ \mu\text{m}^2$ AlGaN/GaN HEMT on Si and diamond substrate for different V_{GS} ranging from $0\ \text{V}$ to $-3\ \text{V}$ by step of $1\ \text{V}$.

As shown in figure 7, a maximum g_m is in the range of $370 \text{ mS}\cdot\text{mm}^{-1}$ for the device on Si substrate while it is decreased in the range of $325 \text{ mS}\cdot\text{mm}^{-1}$ for the same devices transferred to diamond substrate. We also notice in Figure 7, an offset on transfer function and I_{DS} - V_{GS} characteristics. This decrease on g_m and the shift of threshold voltage (and transfer function) could be linked to a piezoelectric stress relaxation which changes the charges in particular under the gate. The process initially optimized on Si substrate can be adapted to get a better advantage on diamond substrate than what is presented in this paper.

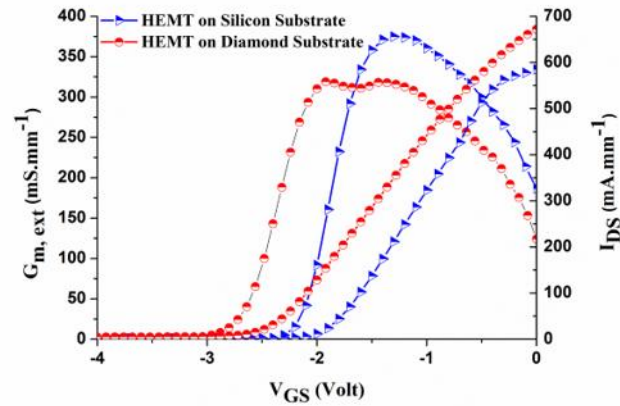


FIG. 7. I_{DS} - V_{GS} and transfer characteristics of AlGaIn/GaN on Si substrate and diamond substrate at $V_{DS} = 4 \text{ V}$.

The scattering parameters S_{ij} are measured from 0.25 GHz up to 67 GHz using a Vector Network Analyzer (VNA) (Agilent Technologies E8361A). The calibration procedure is performed using a Line-Reflect-Reflect-Match (LRRM) calibration procedure. Current gain modulus ($|H_{21}|$) and Mason's unilateral gain (U) are extracted from S-parameters versus frequency measurement. The current gain transition frequency (f_T) and the maximum oscillation frequency (f_{Max}) are directly extracted from the first order linear frequency regression plots (-20 dB/decade) of $|H_{21}|$ and U respectively. For the HEMT

transferred on diamond, at $V_{GS} = -1.75$ V and $V_{DS} = 4$ V, corresponding to the extrinsic transconductance peak, a current gain cut-off frequency f_t of 85 GHz associated with a maximum oscillation frequency f_{max} of 106 GHz are obtained (figure 8).

DC and RF performances have been obtained on 25 devices featuring the same geometry with a low discrepancy in the results (no representative discrepancy on DC results and a discrepancy less than ± 3 GHz on RF results).

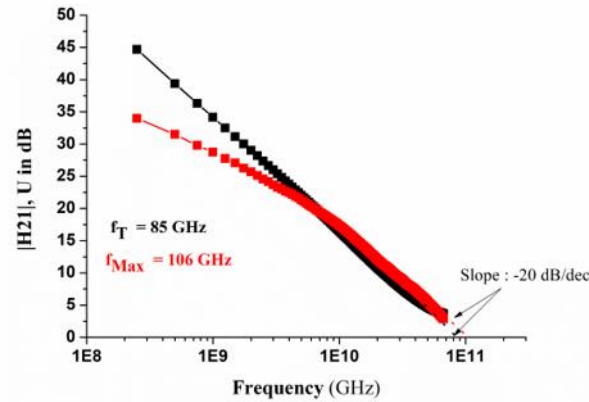


FIG. 8. Current gain modulus $|H_{21}|$ and Mason's unilateral gain (U) versus frequency for a $2 \times 75 \times 0.08 \mu\text{m}^2$ AlGaIn/GaN HEMT on Diamond substrate at $V_{GS} = -1.75$ V and $V_{DS} = 4$ V.

In addition, the decrease of g_m after transfer process of HEMTs from Si to diamond substrate did not significantly decrease the transition frequency f_t (from 87 GHz on Si substrate to 85 GHz on diamond substrate). This can be explained by compensation for this decrease in g_m by a decrease of the capacitances C_{GS} and C_{GD} in the space charge region beneath the gated zone.

IV. SUMMARY AND CONCLUSIONS



This paper details an original way to obtain AlGaIn/GaN HEMTs on diamond substrate through a layer transfer technology at low thermal budget (160°C), using AlN sputtering layers. This new technological method requires an optimization between the crystal structure quality and the thickness of AlN layer, as well as mastering its associated thermal conductivity. Attractive DC and RF performances are demonstrated for a $2 \times 75 \times 0.08 \mu\text{m}^2$ device transferred on diamond substrate. The transistor exhibits a maximum DC current density $I_{\text{DS Max}}$ of $690 \text{ mA}\cdot\text{mm}^{-1}$, a cut-off frequencies $f_{\text{T}} = 85 \text{ GHz}$ and $f_{\text{Max}} = 106 \text{ GHz}$.

Performance can be significantly improved in the future mainly simultaneously addressing two challenges: the improvement of heat dissipation and the reduction of stacking faults in the buffer and stress layer in the AlGaIn/GaN epilayer. In the case of transfer technology, this will go through the use of diamond as host substrate and the use of AlGaIn/GaN epilayer grown on conductive Si substrate or on SiC substrate to obtain a better crystalline quality.

ACKNOWLEDGMENTS

This work was supported by the French Renatech network.

¹ K. R Bagnall, Device-level Thermal Analysis of GaN based Electronics, Master's theses in Mechanical Engineering, Massachusetts Institute of Technology, 2013.

² V. Tilak, B. Green, V. Kaper, H. Kim, T. Prunty, J. Smart, J. Shealy, and L. Eastman, IEEE, Electr. Device. L. **22**, 504 (2001).

³ B. Padmanabhan, D. Vasileska, and S. M Goodnick, Int. Conf. Intell. Syst. (2012).

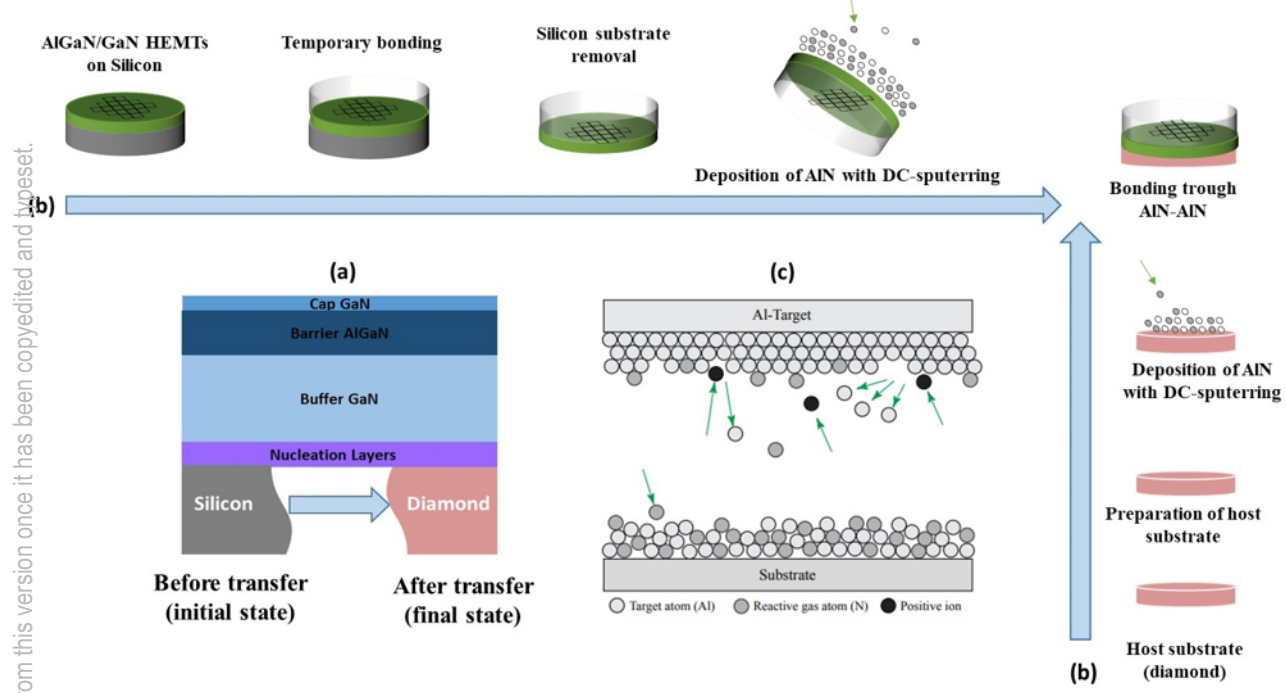
This is the author's peer reviewed, accepted manuscript. However, the online version of record will be different from this version once it has been copyedited and typeset.
PLEASE CITE THIS ARTICLE AS DOI: 10.1116/1.5143418

- ⁴ J.G Felbinger, M.V.S Chandra, S. Yunju, L.F Eastman, J. Wasserbauer, F. Faili, D. Babic, D. Francis, and F. Ejeckam, IEEE. Electr. Device. L. **28**, 948 (2007).
- ⁵ Q. Diduck, J. Felbinger, L.F Eastman, D. Francis, J. Wasserbauer, F. Faili, D.I Babić, and F. Ejeckam, Electron. Lett. **45**, 758 (2009).
- ⁶ Q. Jiang, D. W E Allsopp, and C. R Bowen, J. Phys. D. Appl. Phys. **50**, 165103 (2017).
- ⁷ B. Lu, and T. Palacios, IEEE. Electr. Device. L. **31**, 951 (2010).
- ⁸ J.W Chung, E.L Piner, and T. Palacios, IEEE. Electr. Device. L. **30**, 113 (2009).
- ⁹ G.H Jessen, J. K Gillespie, G. D Via, A. Crespo, D. Langley, J. Wasserbauer, F. Faili, D. Francis, D. Babic, F. Ejeckam, S. Guo, and I. Eliashevich, Compton. IEEE, 271 (2006).
- ¹⁰ P. C Chao, K. Chu, C. Creamer, J. Diaz, T. Yurovchak, M. Shur, R. Kallaher, C. Mcgray, G. D Via, and J. D Blevins, IEEE. T. Electron. Dev. **62**, 3658 (2015).
- ¹¹ T. Liu, Y. Kong, L. Wu, H. Guo, J. Zhou, C. Kong, and T. Chen, IEEE. Electr. Device. L. **38**, 1417 (2017).
- ¹² Q. Wu, Y. Xu, J. Zhou, Y. Kong, T. Chen, Y. Wang, F. Lin, Y. Fu, Y. Jia, X. Zhao, B. Yan, and R. Xu, Ecs. J. Solid. State. Sc. **6**, 171 (2017).
- ¹³ F. Engelmark, AlN and high-k thin films for IC and electroacoustic applications, Doctoral dissertation of Philosophy in Solid State Electronics, Uppsala University, **23**, 2002.
- ¹⁴ P. Altuntas, F. Lecourt, A. Cutivet, N. Defrance, E. Okada, M. Leseq, S. Rennesson, A. Agboton, Y. Cordier, V. Hoel, J. C De Jaeger, IEEE. Electr. Device. L. **36**, 303 (2015).
- ¹⁵ T. S Pan, Y. Zhang, J. Huang, B. Zeng, D. H Hong, S. L Wang, H. Z Zeng, M. Gao, W. Huang, and Y. Lin, J. Appl. Phys. **112**, 044905 (2012).
- ¹⁶ G. A Slack, L. J Schowalter, D. Morelli, and J. A Freitas, J. Cryst. Growth. **246**, 287 (2002).

This is the author's peer reviewed, accepted manuscript. However, the online version of record will be different from this version once it has been copyedited and typeset.
PLEASE CITE THIS ARTICLE AS DOI: 10.1116/1.5143418

- ¹⁷ G. A Slack, R. A Tanzilli, R. O Pohl, and J. W Vandersande, J. Phys. Chem. Solids. **48**, 641 (1987).
- ¹⁸ Y. Zhao, C. Zhu, S. Wang, J. Z Tian, D. J Yang, C. K Chen, H. Cheng, and P. Hing, J. Appl. Phys. **96**, 4563 (2004).
- ¹⁹ S. Bao, K. H Lee, G. Y Chong, E. A Fitzgerald and C. S Tan, Ecs. J. Solid. State. Sc. **4**, 200 (2015).
- ²⁰ M. Alshahed, L. Heuken, M. Alomari, I. Cora, L. Toth, B. Pecz, C. Wachter, T. Bergunde, and J. N Burghartz, IEEE. T. Electron. Dev. **65**, 2939 (2018).

This is the author's peer reviewed, accepted manuscript. However, the online version of record will be different from this version once it has been copyedited and typeset.
PLEASE CITE THIS ARTICLE AS DOI: 10.1116/1.5143418



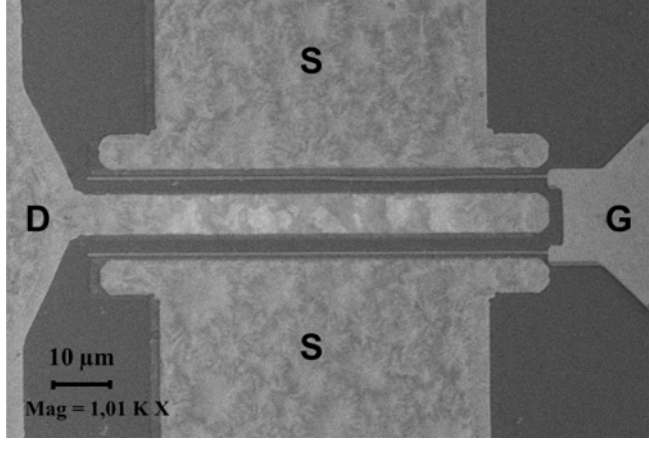


This is the author's peer reviewed, accepted manuscript. However, the online version of record will be different from this version once it has been copyedited and typeset.
PLEASE CITE THIS ARTICLE AS DOI: 10.1116/1.5143418

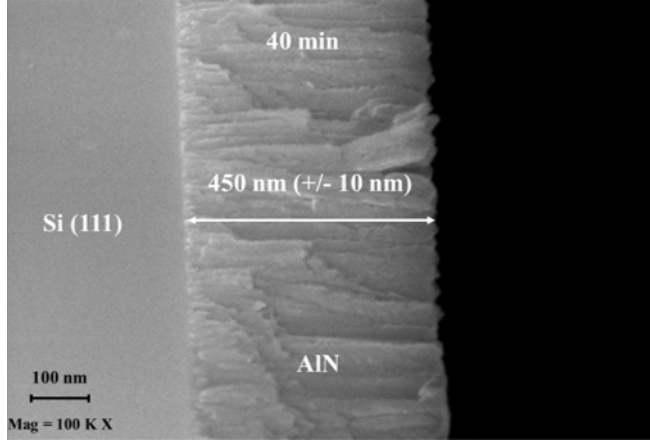




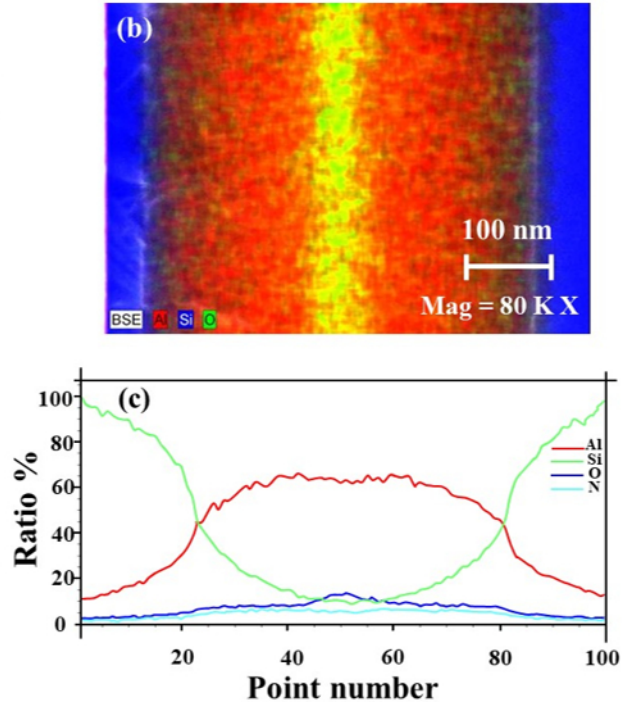
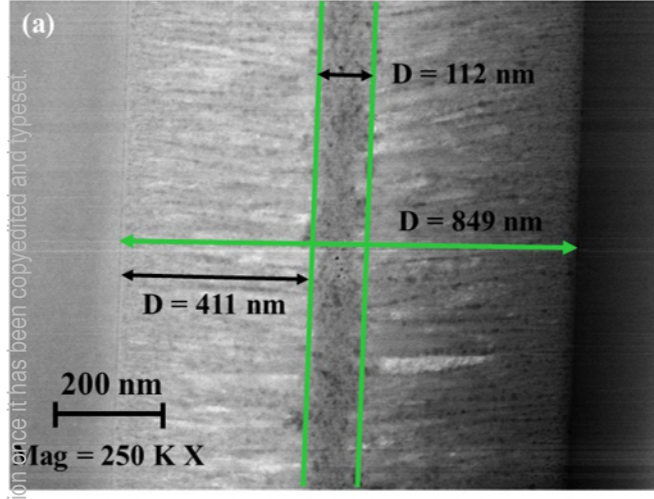
This is the author's peer reviewed, accepted manuscript. However, the online version of record will be different from this version once it has been copyedited and typeset.
PLEASE CITE THIS ARTICLE AS DOI: 10.1116/1.5143418



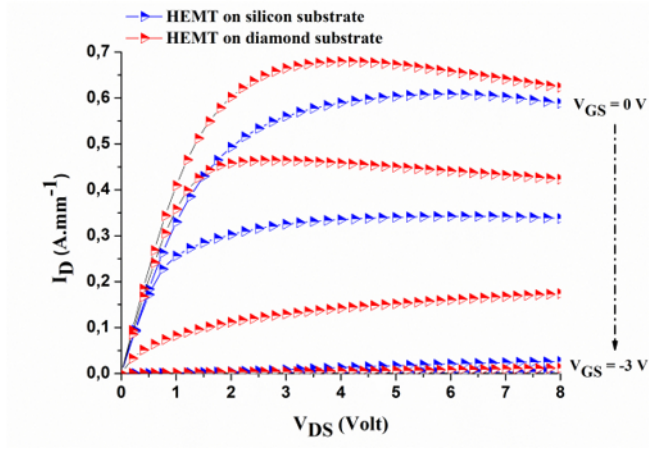
This is the author's peer reviewed, accepted manuscript. However, the online version of record will be different from this version once it has been copyedited and typeset.
PLEASE CITE THIS ARTICLE AS DOI: 10.1116/1.5143418



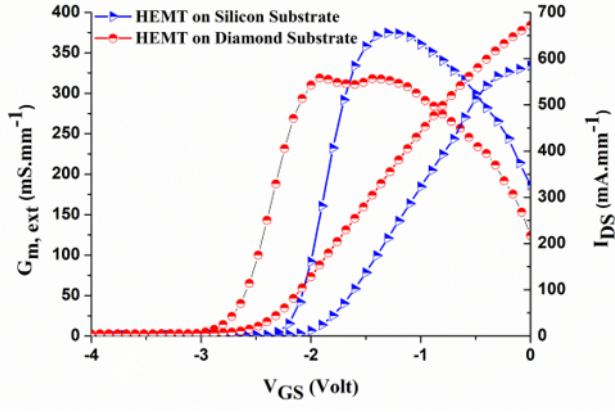
This is the author's peer reviewed, accepted manuscript. However, the online version of record will be different from this version once it has been copyedited and typeset.
PLEASE CITE THIS ARTICLE AS DOI: 10.1116/1.5143418



This is the author's peer reviewed, accepted manuscript. However, the online version of record will be different from this version once it has been copyedited and typeset.
PLEASE CITE THIS ARTICLE AS DOI: 10.1116/1.5143418



This is the author's peer reviewed, accepted manuscript. However, the online version of record will be different from this version once it has been copyedited and typeset.
PLEASE CITE THIS ARTICLE AS DOI: 10.1116/1.5143418



This is the author's peer reviewed, accepted manuscript. However, the online version of record will be different from this version once it has been copyedited and typeset.
PLEASE CITE THIS ARTICLE AS DOI: 10.1116/1.5143418

